Compact Dual-Band CPW-Fed Zeroth-Order Resonant Monopole Antennas

Eugene P. Jee, *Student Member, IEEE*, and Yong Jee, *Member, IEEE*

***Abstract*—A compact dual-band coplanar waveguide (CPW)-fed monopole antenna loaded with a split-ring resonator is presented in this letter. The split-ring resonator is shunt-connected to the folded monopole and has generated a shunt capacitance or inductance as an electrically small resonator yielding a zeroth-order resonant monopole. The proposed antenna has a length of 0.062 wavelengths and a width of 0.06 wavelengths and exhibited −10-dB impedance bandwidths of 50 MHz at 1780 MHz and 1120 MHz at 3440 MHz. The radiation patterns show a dipole-like mode at 1710 MHz and a monopole-like one at 3820 MHz. The measured radiation efficiencies are measured as 17% at 1710 MHz and 88% at 3820 MHz.**

***Index Terms*—Coplanar waveguides (CPWs), monopole antennas, split-ring resonators (SRRs), zeroth-order resonators.**

I. Introduction

WHEN resonators employ the property of zero or negative propagation constant embedded in a monopole antenna, resonators can have an infinite resonant wavelength that is independent of the size of the resonator [1]. The idea of materials with both negative electrical permittivity and magnetic permeability was first introduced by Veselago [2]. Pendry *et al.* suggested split-ring resonators (SRRs) that exhibit a negative magnetic permeability around magnetic resonance frequency [3]. However, it is difficult to design the topology of the SRRs as compact zeroth-order resonant (ZOR) antennas. Numerous composite right/left-handed transmission line (CRLH-TL) structures included different types of shunt reactive elements, such as interdigital capacitors, gap capacitors, or parallel-plate capacitors, on their compact-size antennas to produce CRLH-TL unit cells [2]–[7].

In this letter, we propose a coplanar waveguide (CPW)-fed zeroth-order resonant monopole antenna with installing an SRR on the monopole. The electric and magnetic resonances can be excited along the loop of a SRR, and then magnetic fields perpendicular to the SRR plane and, correspondingly, negatively or positively directed propagation waves parallel to the plane [2].

Manuscript received March 21, 2012; revised May 10, 2012; accepted June 07, 2012. Date of publication June 19, 2012; date of current version July 06, 2012. This work was supported by Sogang University under Research Grant No. 200911014 and the Basic Science Research Program through the National Research Foundation of Korea (NRF) funded by the Ministry of Education, Science and Technology under Grant No. 2012R1A1A2001131.

The authors are with the Department of Electronic Engineering, Sogang University, Seoul 121-742, Korea (e-mail: eugenej@uw.edu; yongj22@sogang.ac.kr).

Color versions of one or more of the figures in this letter are available online at http://ieeexplore.ieee.org.

Digital Object Identifier 10.1109/LAWP.2012.2205212

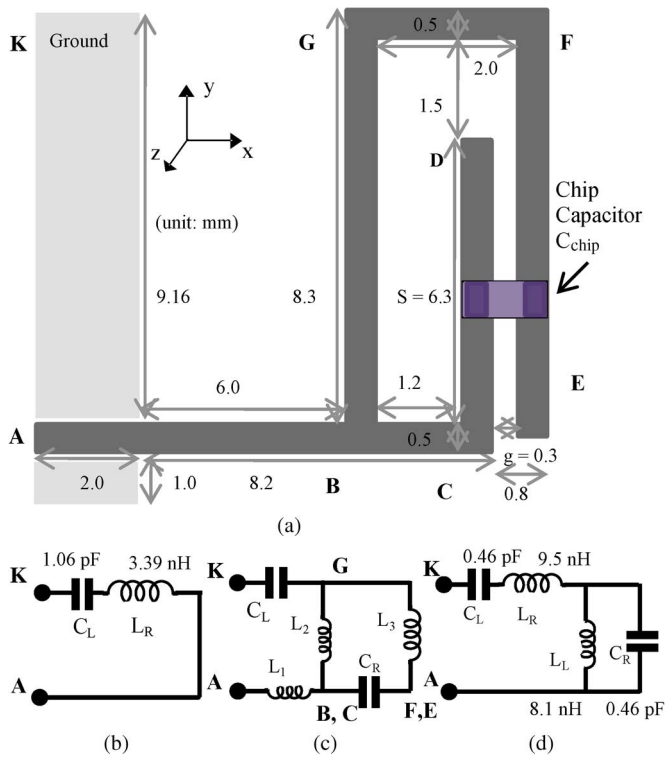

Fig. 1. Geometrical configuration of proposed CPW-fed ZOR monopole antenna. (a) Geometry. (b) Conceptual LC equivalent circuit model of a monopole antenna. (c) Equivalent circuit of a CRLH-TL cell. (d) Equivalent circuit of a CPW-fed ZOR monopole antenna loaded with a chip capacitor.

The monopole resonators thus operate in a zeroth-order mode, not in the conventional resonator mode. Such antennas yield lower resonance frequencies than those of normal monopoles, along with good input impedance matching and radiation efficiency, showing a reduction in the antenna size.

II. Antenna Design

Fig. 1(a) shows the geometrical configuration of a proposed antenna based on a folded monopole. The length of the monopole (path ABGFE) of Fig. 1(a) was chosen based on the design guideline that the lowest resonance can be selected where the length is approximately $0.25\lambda_0$ and the monopole has one oscillating electromagnetic field of an open-ended resonator, where λ_0 is the free-space wavelength in terms of the lowest operating frequency. The length of the monopole in this design is 28 mm corresponding to the resonant frequency of 2679 MHz. The conceptual LC equivalent circuit of the monopole antenna provides an intrinsic series capacitance

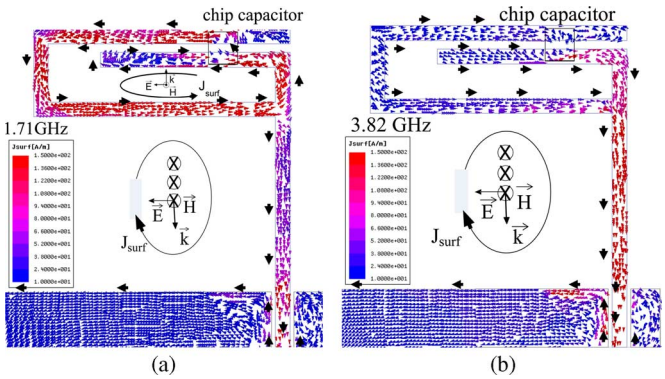

Fig. 2. HFSS-simulated surface current distribution on the pattern of ZOR monopole antenna with 0.6-pF capacitor. (a) 1710 MHz. (b) 3820 MHz.

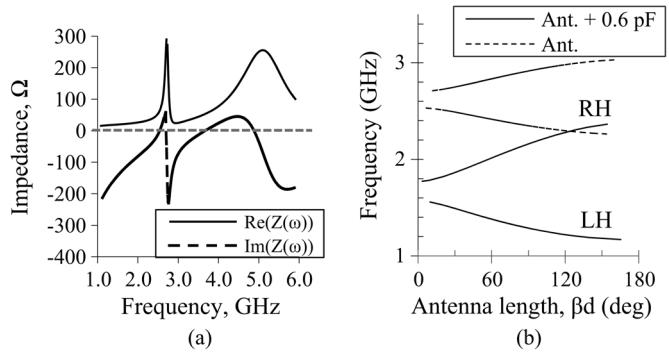

Fig. 3. (a) Simulated impedance curve. (b) Dispersion diagrams of CRLH-TLs on CPW-fed ZOR antenna structures.

$C_{\rm L} = 1.06$ pF and an inductance $L_{\rm R} = 3.39$ nH from the monopole, as shown in Fig. 1(b).

In the derivation of LC parameters, we have calculated inductance and capacitance by using HFSS-simulated Z impedance parameters and the following equations: resonant frequencies $\omega_0 = 1/\sqrt{L_{\rm L}C_{\rm R}}$; antenna's quality factor $Q_{\rm ant} = \omega_0/{\rm BW}_{\text{3-dB}} = R\sqrt{C_{\rm R}/L_{\rm L}}$; 3-dB bandwidth; HFSS simulated ${\rm BW}_{\text{3-dB}}$; input port resistance R; and measured S_{11} data.

A single SRR can be formed simply by inserting a split current loop (path BGFEDCB) into the monopole. The loop and the gap located along the parallel strips of paths CD and EF in Fig. 1(a) provide an inductance and a gap capacitance. By suitably adjusting dimensions of the loop and the gap, an SRR is loaded on the folded monopole. The geometry generates magnetic resonances around the frequency of 2400 MHz.

Note the surface current distribution observed from the full-wave numerical analysis in Fig. 2. It shows that the current wave has magnetic resonance modes of half-wavelength inside an SRR where there are two concentric conductor edge-rings with gap, along the current path BGFEDCB. If electric fields are applied along the positive y-axis direction of the antenna, surface current $J_{\rm surf}$ is generated on the loop of path BCEFG in the positive y-axis direction, and the magnetic field H in the positive z-axis direction, which is perpendicular to the SRR plane as shown in Fig. 2(a). The wave propagation is then formed along the positive x-axis direction of the wave vector that is parallel to the SRR plane, as expected. In the loop ABGK, likewise, the wave propagation direction is in the negative x-axis at a lower resonant frequency of 1710 MHz.

However, at a higher resonant frequency of 3820 MHz, the antenna operates as a normal monopole mode. There is no positive-x-axis-directed wave propagation, as shown in Fig. 2. Here, a common element to provide magnetic responses is the SRR.

The loop of the SRR path BGFEDCB is thus a resonator that couples to a perpendicular magnetic field and can be characterized by the effective capacitance C of the gap and the effective inductance L of the loop defined by the path BGFEDCB. It can be shown in terms of a resonant LC circuit with a resonance frequency, $\omega_m = 1/\sqrt{L_{\rm L}C_{\rm R}}$. The electromagnetic resonant response of the loop current in an SRR may be represented as series-LC-equivalent circuits that include C, L_3, where C and L_3 are parallel to L_2, as shown in Fig. 1(c).

The conceptual equivalent circuit consists of the series capacitor C_1; the inductors L_1, L_2, and L_3; and the shunt capacitor C, as shown in Fig. 1(c). The series capacitor C_1 has been formed by a monopole strip and ground patches, the inductors L_1, L_2, and L_3, implemented by the inductive strip (path ABGF), and the shunt capacitor C by the gap between the strips CD and EF.

The resultant LC equivalent circuit represents a CRLH-TL unit-cell loaded monopole. Fig. 1(d) depicts the redrawn equivalent circuit of a CRLH-TL cell that is composed of a series capacitance $C_{\rm L}$ and inductance $L_{\rm R}$, as well as shunt gap capacitance $C_{\rm R}$ and inductance $L_{\rm L}$. Based on the circuit, we can examine the input emittances at the port of the antenna given by the equation

$$Z_{\rm series} = j\left\{\omega\left(L_{\rm R} + \frac{L_{\rm L}}{(1-\omega^2 C_{\rm R}L_{\rm L})}\right) - \frac{1}{\omega C_{\rm L}}\right\},$$
$$Y_{\rm shunt} = j\left(\omega C_{\rm R} - \frac{1}{\omega L_{\rm L}}\right). \quad (1)$$

The characteristic impedance is provided by $Z_{\rm C} = \sqrt{Z_{\rm series}/Y_{\rm shunt}}$. The resonant frequencies are given by that of series circuit $\omega_{\rm se} = 1/\sqrt{C_{\rm L}L_{\rm R}^{\rm E}} = 1/\sqrt{C_{\rm L}(L_{\rm R} + L_{\rm L}/(1-\omega^2 C_{\rm R}L_{\rm L}))}$ and that of shunt circuit $\omega_{\rm sh} = 1/\sqrt{L_{\rm L}C_{\rm R}}$, where the effective series inductance $L_{\rm R}^{\rm E} = (L_{\rm R} + L_{\rm L}/(1-\omega^2 C_{\rm R}L_{\rm L}))$. The shunt capacitor $C_{\rm R}$ makes it possible for the monopole antenna to lower its resonant frequencies, $\omega_{\rm se}$ and $\omega_{\rm sh}$, while supporting the miniaturization of the antenna. The resultant antenna in this design formed by the insertion of a gap capacitor into the monopole shifts the resultant series resonant frequency to 2410 MHz following the effective inductance, $L_{\rm R}^{\rm E}$, and also generated another shunt resonant frequency of 2679 MHz by the shunt circuit of $L_{\rm L}$ and $C_{\rm R}$. The behavior of an impedance Z-curve is illustrated in Fig. 3(a)

The propagation constant $\gamma \cdot \ell$ of a transmission line is given by $\gamma \cdot \ell = (\alpha + j\beta) \cdot \ell \approx j\beta \cdot \ell = \sqrt{Z_{\rm series}/Y_{\rm shunt}}$ where α is the attenuation constant, β the phase constant, and ℓ the length of the unit cell. In a CRLH lossless TL, where an SRR is applied into the monopole antenna, the propagation constant can be purely imaginary so that $\gamma = j\beta\ell$. A passband exists in the frequency range when β is purely real, while a stopband appears

when β is purely imaginary. Thus, the range of a passband from $\omega_{\rm se}$ to $\omega_{\rm sh}$ depends on the shunt capacitance $C_{\rm R}$.

A dispersion diagram of a CRLH-TL can be provided by applying the Bloch and Floquet theory as follows [1]:

$$\beta \cdot \ell = \cos^{-1}\left(1\frac{\left(\omega_2 - \omega_{\rm se}^2\right)\left(\omega^2 - \omega_{\rm sh}^2\right)}{2\omega^2\omega_{\rm R}^2}\right). \quad (2)$$

where β becomes the propagation constant for Bloch waves, and $\omega_{\rm R} = 1/\sqrt{C_{\rm L}L_{\rm L}C_{\rm R}L_{\rm R}}$. Through HFSS simulation, we can see the dispersive curve of having both negative and positive values of propagation constant β, as plotted in Fig. 3(b).

Note that the input impedance of the antenna exhibits a similar behavior as the one shown in Fig. 3(a). The monopole antenna is an open-ended resonator, and the load impedance $Z_{\rm L}$ becomes infinite in this topology. As β approaches to zero, where the frequency $\omega > \omega_{\rm sh}$, the input impedance $Z_{\rm input}^{\beta\to 0,\omega>\omega_{\rm sh}}$ of the antenna goes to infinite showing a bandstop at 2660 MHz as follows:

$$\begin{aligned} Z_{\rm input}^{\beta\to 0,\omega>\omega_{\rm sh}} &= Z_{\rm C}\frac{Z_{\rm L}jZ_{\rm C}\tan\beta\ell}{Z_{\rm C}+jZ_{\rm L}\tan\beta\ell}\Bigg|_{Z_{\rm L}\to\infty}^{\beta\to 0} \\ &\approx Z_{\rm C}\frac{1}{j\beta\ell} = \frac{1}{Y_{\rm shunt}} = \frac{jL_{\rm L}}{1-\omega^2 C_{\rm R}L_{\rm L}}. \end{aligned} \quad (3)$$

When β approaches to zero where the frequency $\omega < \omega_{\rm se}$, the circuit instead has a short circuit at the resonant frequency $\omega_{\rm se}$, and the input impedance in (1) becomes zero with the radiator excited at 2410 MHz: $Z_{\rm input}^{\beta\to 0,\omega<\omega_{\rm se}} = Z_{\rm series}/Y_{\rm shunt} = 0$. Near the band-gap of Fig. 3(b), the propagation constant becomes zero.

While we were able to estimate the effect of the shunt capacitance $C_{\rm R}$, because $C_{\rm R}$ lowers the resultant resonant frequency $\omega_{\rm sh}$ of the antenna, a limitation exists on increasing the shunt capacitance $C_{\rm R}$ in this topology. The maximum available capacitance is limited to 0.47 pF because the gap capacitor formed by the parallel strips CD and EF is 0.062 pF/mm and the maximum length of strip CD 7.5 mm.

In order to further lower the resultant resonance frequency, we have substituted to implant another type of additional capacitance. When a chip capacitor of 0.6 pF is added, the shunt capacitance of the circuit becomes 1.07 pF, and the antenna shifts the shunt resonant frequency to 1710 MHz. In this case, the antenna forms a short circuit at the frequency of 1570 MHz and generates an open circuit at 1780 MHz that realizes a stopband showing a characteristic of a narrow bandwidth.

When operating in a regular monopole mode, the antenna functions as a two-branch monopole [7], i.e., along the path ABGFE and ABCD, and shows a resonant frequency range from 2870 to 3960 MHz. When operated in a ZOR mode, the antenna excites the lower resonant frequency around 2410 MHz, revealing an equivalent circuit with the parameters of $C_{\rm L} = 0.46$ pF, $L_{\rm R} = 9.3$ nH, $C_{\rm R} = 0.50$ pF, and $L_{\rm L} = 7.36$ nH.

III. Experimental Measurements

The pattern has been printed on a 0.6-mm-thick, low-cost FR-4 material with a 9-μm-thick copper metal. The relative dielectric constant of a substrate $\varepsilon_{\rm r}$ is 4.4, and loss tangent is 0.002. The CPW feed has a width of 0.5 mm and a gap of 0.142 mm and is connected to a 50-Ω SMA connector across the ground planes. Fig. 4 shows the measured S_{11} of the proposed antenna. The antenna shows a behavior of dual-frequency-band excitation. The 28-mm-long monopole itself excites the measured resonant frequency at 3440 MHz with a -10-dB bandwidth of 730 MHz (3250–3980 MHz). The antenna generates another resonant frequency at 2570 MHz after loading a distributed gap capacitor. The measured -10-dB bandwidths of S_{11} show 250 MHz (2410–2660 MHz) to cover the Digital Communication Systems (DCS) band and 730 MHz (3250–3980 MHz) to cover the WiMAX band. When two 0.3-pF chip capacitors (Murata GRM1555C1HR30BZ01) were attached, the chip-capacitor loaded SRR (L-SRR) antenna shifts the resonance frequency to the dual range of 1750–1800 and 2860–3980 MHz. The design size of the antenna becomes $11 \times 10.8 \times 0.6$ mm^3, which is equivalent to $0.062\lambda_0 \times 0.060\lambda_0 \times 0.00034\lambda_0$.

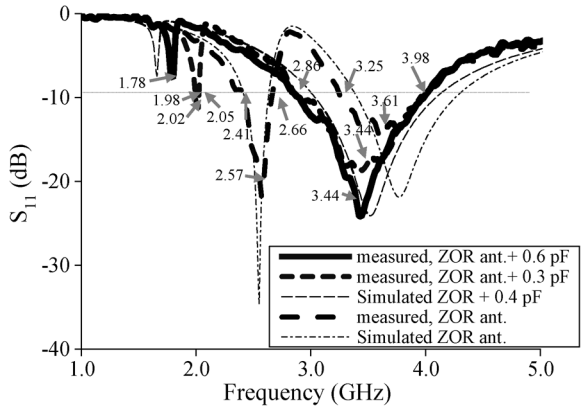

Fig. 4. Measured S_{11} of proposed CPW-fed ZOR monopole antennas.

The performance of an antenna is generally degraded with its size reduction at the expense of radiation efficiency and bandwidths. In this design, $Q_{\rm ant}$ of the antenna can be obtained based on the frequency response. The proposed monopole has the quality factor $Q_{\rm ant}$ of 36 at 1710 MHz and 27 at 3440 MHz. The Wheeler limit [4], [8] for quality factor can be given by the equation: $Q_{\rm Wheeler} = (9/2)/(1.87 \cdot (k \cdot r_{\rm e})^3)$, where k the wavenumber is associated with the electromagnetic field, $r_{\rm e}$ the radius of a sphere enclosing the antenna, and 1.87 the Fringing Factor [8]. The Harrington limit [8] for antenna gain is given by the equation: $G_{\rm Harrington} = (k \cdot r_{\rm e})^2 + 2k \cdot r_{\rm e}$. The Harrington limit defines the limit for the highest achievable gain of an electrically small antenna that can be enclosed within a sphere of effective radius [4]. Since the antenna size of the proposed structure is 11×10.8 mm^2 and the $r_{\rm e}$ 7.71 mm, $k \cdot r_{\rm e} = 0.291$ and 0.555 at 1710 and 3440 MHz, and $G_{\rm Harrington} = -1.77$ and 1.52 dB, $Q_{\rm ant}/Q_{\rm Wheeler} = 0.37$ and 1.93, respectively. The measured antenna gains are -5.2 dBi at 1710 MHz and 1.97 dBi at 3820 MHz. The fractional bandwidth (FBW) of the antenna is given by the equation $\mathrm{FBW}_{\text{3-dB}} = 1/(R \cdot C_{\rm R})$, and the FBWs of the L-SRR antenna are 2.8% and 32.6% at 1780 and 3440 MHz, respectively.

Radiation efficiency (RE) was measured with the equation: $\mathrm{RE} = 10^{\mathrm{Gain}/10}/\mathrm{Directivity}$, $\mathrm{Directivity} = 41,253/\mathrm{HP_H} \cdot \mathrm{HP_E}$, where Gain is the maximum gain in decibels, $\mathrm{HP_H}$ the

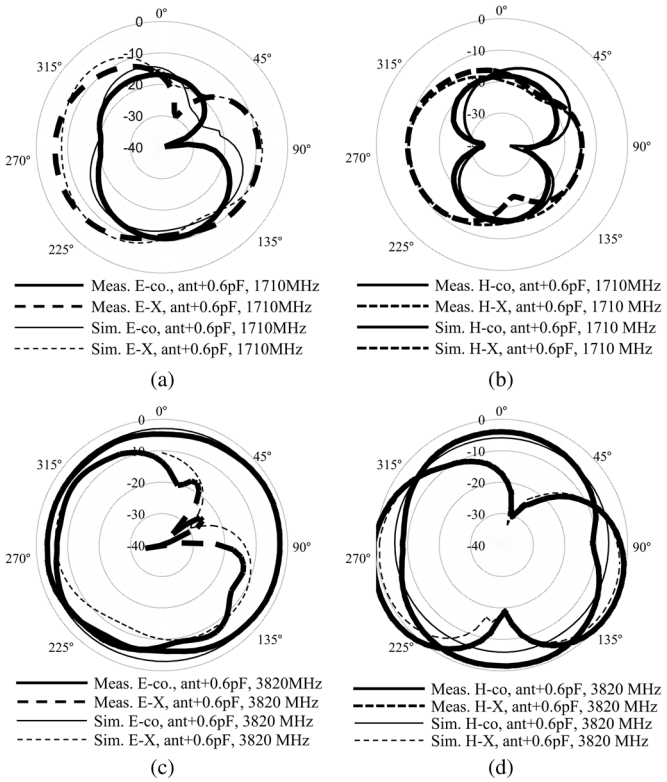

Fig. 5. Measured and HFSS-simulated radiation patterns of CPW-fed ZOR antennas loaded with 0.6-pF chip capacitor. (a) E-field co- and cross-polarization patterns at 1710 MHz. (b) H-field co- and cross-polarizations pattern at 1710 MHz. (c) E-field co- and cross-polarization patterns at 3820 MHz. (d) H-field co- and cross-polarization patterns at 3820 MHz.

half-power beamwidth of H-field, and $\mathrm{HP_E}$ that of E-field in degrees. The parameters were measured in an anechoic chamber.

Measured REs on a chip-capacitor unloaded SRR (U-SRR) monopole antenna originally showed 17.2% at 1710 MHz, 85.9% at 2680 MHz, and 81.2% at 3820 MHz. Measured REs on an L-SRR antenna instead showed 17.1% at 1710 MHz, 83.1% at 2680 MHz, and 88.3% at 3820 MHz. High RE was obtained on the SRR structure having a planar topology at 3820 MHz. However, the RE of the L-SRR antenna at 1710 MHz did not improve, showing the same level as those of the U-SRR antenna. We could not improve the antenna gain of the L-SRR with increasing the numerical value of capacitance through the addition of lumped chip capacitors and without changing the radiation area, while the antenna's magnetic resonant frequencies lowered due to the proposed antenna's structural limitations.

The radiation patterns show a dipolar fashion at 1710 MHz and an omnidirectional one at 3820 MHz, as shown in Fig. 5. The measured data are compared to the data of another report in Table I.

TABLE I
MEASURED AND THEORETICAL VALUES FOR RESONANT FREQUENCY, Q, ANTENNA GAINS, RADIATION EFFICIENCIES

Ref.	f_{res} (GHz)	Rad. Eff. (%)	Ant. Size (mm^3)	Q_{ant}/Q_{whleer}	Ant. Gain (dBi)	$K \cdot r_e$	FBW (%)
Prop. Ant.	1.71	17.2 %	11 x 10.8 x 0.6	0.37	-5.2	0.29	2.8
	3.68	88.3 %		1.93	1.97	0.56	32.6
Zhu [4]	2.45	67.4 %	20 x 23.5 x 1.5	5.60	1.14	0.79	3.6
	3.50	86.3 %		0.44	1.15	0.56	16.9
	5.50	85.3 %		7.90	1.78	0.89	28.9

IV. CONCLUSION

We have presented a CPW-fed monopole antenna loaded with a split-ring resonator in this letter. The property of a split-ring resonator has provided CPW-fed monopoles with the construction of dual resonant zeroth-order resonators. The fabricated prototype with a size of $0.060\lambda_0 \times 0.062\lambda_0 \times 0.0034\lambda_0$ has provided -10-dB bandwidths of 50 MHz at 1780 MHz and 1120 MHz at 3440 MHz. The radiation efficiency for the proposed antenna showed 17.1% at 1710 MHz and 88.3% at 3820 MHz. The ability of creating an SRR structure within a CPW-fed monopole can greatly relax the restrictions imposed upon the design of compact antenna systems such as multiband and software-defined radio wireless systems.

REFERENCES

[1] A. Lai, T. Itoh, and C. Caloz, "Composite right/left-handed transmission line metamaterials," *IEEE Microw. Mag.*, vol. 5, no. 3, pp. 34–50, Sep. 2004.
[2] V. G. Veselago, "The electrodynamics of substances with simultaneously negative values of ε and μ," *Sov. Phys. Usp.*, vol. 10, no. 4, pp. 509–516, Apr. 1968.
[3] J. Pendry, A. Holden, D. Robbins, and W. Stewart, "Magnetism from conductors and enhanced nonlinear phenomena," *IEEE Trans. Microw. Theory Tech.*, vol. 47, no. 11, pp. 2075–2084, Nov. 1999.
[4] J. Zhu, M. A. Antoniades, and G. V. Eleftheriades, "A compact tri-band monopole antenna with single-cell metamaterial loading," *IEEE Trans. Antennas Propag.*, vol. 58, no. 4, pp. 1031–1038, Apr. 2010.
[5] T. Jang, J. Choi, and S. Lim, "Compact coplanar waveguide (CPW)-fed zeroth-order resonant antennas with extended bandwidth and high efficiency on via less single layer," *IEEE Trans. Antennas Propag.*, vol. 59, no. 2, pp. 363–372, Feb. 2011.
[6] Y. Horii, C. Caloz, and T. Itoh, "Super-compact multilayered left-handed transmission line and diplexer application," *IEEE Trans. Microw. Theory Tech.*, vol. 53, no. 4, pp. 1527–1534, Apr. 2005.
[7] S. Baek and Y. Jee, "Compact integrated monopole antenna with CPW-fed meander resonators," *Electron. Lett.*, vol. 47, no. 2, pp. 79–80, 2011.
[8] T. Milligan, "Antenna designer's notebook," *IEEE Antennas Propag. Mag.*, vol. 50, no. 2, pp. 130–131, Apr. 2008.
[9] C.-J. Lee, K. M. K. H. Leong, and T. Itoh, "Composite right/left-handed transmission line based compact resonant antennas for RF module integration," *IEEE Trans. Antennas Propag.*, vol. 54, no. 8, pp. 2283–1038, Aug. 2006.